

NRL Report 4194

**VIRTUAL SOURCE LUNEBERG LENSES**

**G.D. Peeler, K.S. Kelleher, and H.P. Coleman**

**Antenna Research Branch  
Radio Division I**

July 13, 1953

**NAVAL RESEARCH LABORATORY  
WASHINGTON D.C.**

**APPROVED FOR PUBLIC  
RELEASE - DISTRIBUTION  
UNLIMITED**



## ABSTRACT

The portion of a spherical Luneberg lens contained between two plane reflectors has been investigated as a lens of reduced size and weight. If the reflectors pass through the center of the sphere, the resulting system produces several perfectly focused radiation beams, each appearing to originate from a virtual source on the surface of the full sphere. The virtual source positions and the position, beamwidth, and gain of the beams are accurately predicted from the spherical wedge angle and the source position. When the wedge angle is  $\pi/p$ , where  $p$  is an integer, rays with  $p$  reflections form the beam having the greatest gain and a displacement from the wedge bisector equal to the source displacement. For applications in which only this principal beam is desired, the gain of the unwanted beams can be reduced by absorption, reflection, or illumination taper.

Scanning is achieved by moving the feed along the surface of the spherical wedge; if  $p$  is an odd integer, scanning can be obtained by moving the wedge past a fixed feed.

Experimental data were taken on a two-dimensional X-band model having a value of  $p = 1$ . Good agreement was found with the predicted performance regarding beam position, beamwidth, and gain. The single, undesired beam was minimized by the use of absorbing material.

## PROBLEM STATUS

This is an interim report; work on the problem is continuing.

## AUTHORIZATION

NRL Problem 34R09-56  
RDB Project NE 121-021

Manuscript submitted June 5, 1953

## VIRTUAL SOURCE LUNEBERG LENSES

### INTRODUCTION

Within recent years workers in microwave optics have given the Luneberg lens<sup>1</sup> much attention as a wide-angle scanning antenna because of its complete symmetry. No consideration, however, has been given to the utilization of only a portion of this lens, together with proper reflecting surfaces, as a means of reducing its size and weight. This combination of the lens section and the reflectors will be called a virtual source Luneberg lens. In this report, some of the general properties of these Luneberg lenses are considered, and experimental data are presented for a lens of this type.

The Luneberg lens is a spherical, variable-index-of-refraction system in which, for a unit-radius lens, the index of refraction  $n$  varies with the distance from the center  $r$  as  $n = \sqrt{2 - r^2}$ . In this discussion, it is both convenient and sufficient to consider rays in a plane through the source and the lens center and if necessary, to extend these considerations to the full lens. As shown in Figure 1, rays which leave the source  $S$  on the surface of the lens are focused into parallel rays. A ray leaving the source at an angle  $\psi$  from the diameter  $ST$  is radiated from the lens at the point  $P$  so that the radius  $OP$  forms an angle  $\psi$  with  $ST$ . The ray which leaves the source at  $\psi = 0$  propagates in a straight line through the center, while a ray leaving at  $\psi = \pm \pi/2$  propagates along one fourth of the lens circumference before being radiated.

### VIRTUAL SOURCE LENSES

Because of symmetry in the Luneberg lens, plane reflecting surfaces may be placed through its center and the ray paths may be traced by the use of images. Consider a source at  $S$  (Figure 2) displaced from the reference axis  $RO$  by an angle  $\beta$  (positive angles are measured counterclockwise). The addition of a single reflector perpendicular to  $RO$  will produce a virtual source. A typical ray, leaving  $S$  at an angle  $\psi$ , propagates through the lens and is reflected at this surface so that the angle of reflection equals the angle of incidence. This ray continues to propagate as if it originated at the virtual source  $S_1$ , which is the mirror image of  $S$  in the reflector

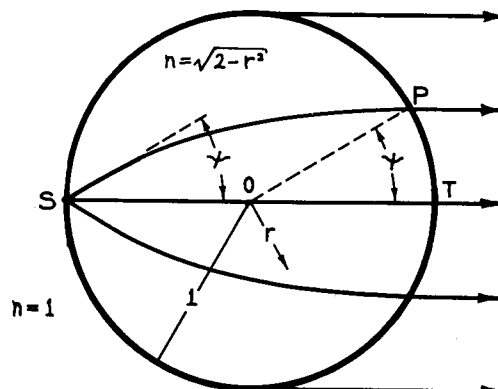


Figure 1 - Rays in a Luneberg lens

<sup>1</sup>Luneberg, R. K., "Mathematical Theory of Optics," Brown University Graduate School, Providence, R. I., 1944

( $S_1$  is displaced from RO through an angle  $\pi - \beta$ ). Therefore, all reflected rays are focused into a beam of parallel rays which is displaced at an angle  $-\beta$  from RO as if the real source, in a full lens, were at  $S_1$ . If  $\beta \neq 0$ , some of the rays will be radiated without reaching the reflector and a focused beam of these "direct" rays is formed in the direction of SO.

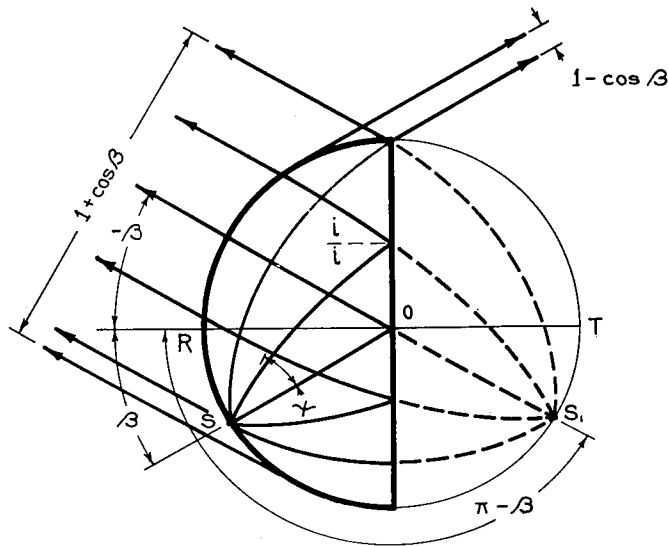


Figure 2 - Rays in a one-reflector virtual source Luneberg lens

This example is a special case of a spherical wedge in which the wedge angle is  $\pi$ . A general spherical wedge of angle  $\alpha$  (Figure 3) can also be examined by employing virtual sources. In this figure, the reference axis RO bisects the wedge angle and the source S is displaced from RO by an angle  $\beta$ . If  $\alpha > \pi/2$  and  $|\beta| + \alpha/2 > \pi/2$ , a direct beam is formed; if  $\alpha < \pi/2$ , all rays are reflected and there is no direct beam. Figures 3a and 3b show an arrangement with  $\alpha > \pi/2$  and  $|\beta| + \alpha/2 < \pi/2$ . Let  $\psi_1$  be a boundary angle between two groups of rays leaving the source. In Figure 3a, rays at angles  $\psi$  from SO, such that  $-\pi/2 \leq \psi < \psi_1$ , are reflected from the lower reflector and are radiated from the lens as if they originated at the virtual source  $S_1$ . As shown in Figure 3b, rays leaving S at angles  $\psi$ , such that  $\psi_1 < \psi < 0$  also reflect from the lower reflector, propagate as if they originated at the virtual source  $S_1$ , reflect from the upper reflector, and are radiated from the lens at an angle  $\pi + 2\alpha + \beta$ . Apparently, the radiated beam has been produced by the virtual source  $S_3$  at an angle  $2\alpha + \beta$ . By similar reasoning it can be shown that rays leaving S for positive values of  $\psi$  produce a virtual source  $S_2$  at an angle  $-(\alpha + \beta)$  and the corresponding radiation beam at an angle  $\pi - (\alpha + \beta)$ .

For any wedge angle  $\alpha$ , similar techniques may be used to show that all the rays are radiated into perfectly focused beams as if they originated from their respective virtual sources. Table 1 contains a summary of virtual source and beam positions in terms of  $\alpha$  and  $\beta$ . Notation for the virtual sources is given so that the order of their positions from S on a circumference of the full sphere is  $S_1, S_3, S_5, \dots$  in the positive direction and  $S_2, S_4, S_6, \dots$  in the negative direction. If  $\alpha$  is small, the beams that might be formed by rays with few reflections are not radiated; the corresponding virtual source positions, however, are useful in determining the ray paths. For a given  $\alpha$ , there is a maximum number of reflections so that a finite number of radiated beams exists.

An idea of the relative gains of these beams may be obtained by noting that the beams formed from rays leaving the feed at large angles from the central ray are radiated from

relatively small apertures and produce relatively large beamwidths. Also, owing to the illumination taper of a normal feed, these beams contain relatively little energy. The combination of these effects considerably reduces the gain of such beams, and as a result, the beams formed from rays leaving the feed at small angles from the central ray are the most important ones. Henceforth, the beam with the greatest gain will be referred to as the principal beam.

The most useful and interesting of these lenses are those which produce the principal beam at either  $\pm \beta$  i.e., with the principal beam displacement from RO equal to the source displacement. This condition is achieved if  $\alpha = \pi/p$ , where p is an integer equal to the maximum number of reflections for any ray. Proof of this statement may be seen by examining the position of the beams formed from rays with p reflections. When  $\alpha = \pi/p$ , the virtual sources  $s_{2p-1}$  and  $s_{2p}$  coincide at the position  $\pi + (-1)^p \beta$  to yield the principal beam at  $-\beta$  for p odd and  $+\beta$  for p even, so that there are  $2p-1$  virtual sources. In order to calculate the minimum number of reflections for any ray, one notes that the circumferential ray must traverse a  $90^\circ$  arc before being radiated; this number is  $p/2$  for p even and  $(p-1)/2$  for p odd (except for  $(p+1)/2$  when  $\beta = 0$ ). There are  $p+1$  radiation beams, except when p is odd and  $\beta = 0$ ; in this event, there are p beams.

Some physical insight into the behavior of these lenses can be obtained by examining

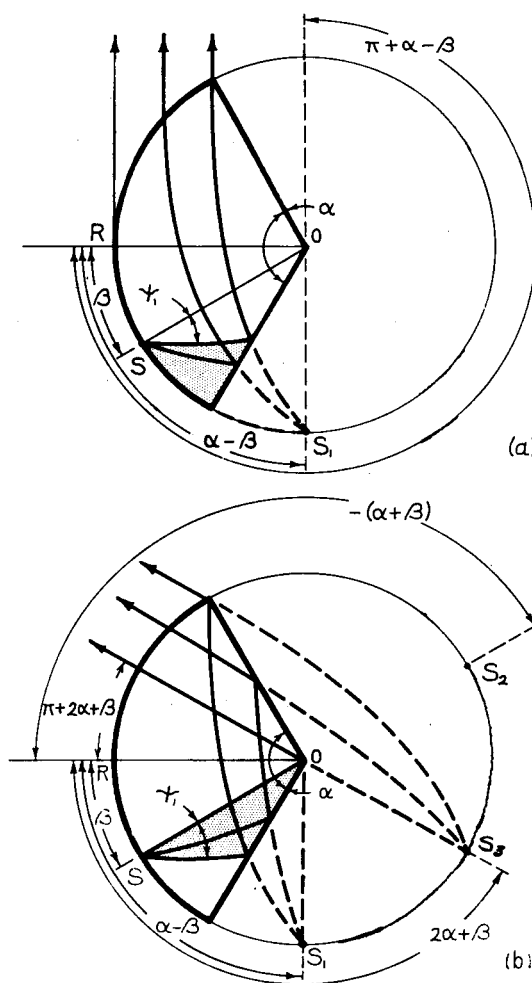


Figure 3 - Rays in a two-reflector virtual source Luneberg lens

TABLE 1  
Virtual Source and Beam Positions

Beam Formation	Virtual Source	Virtual Source Position	Radiated-Beam Position
Direct	$s^*$	$\beta$	$\pi + \beta$
Rays with one reflection	$s_1$	$\alpha - \beta$	$\pi + \alpha - \beta$
	$s_2$	$-(\alpha + \beta)$	$\pi - (\alpha + \beta)$
Rays with two reflections	$s_3$	$2\alpha + \beta$	$\pi + 2\alpha + \beta$
	$s_4$	$-(2\alpha - \beta)$	$\pi - (2\alpha - \beta)$
Rays with three reflections	$s_5$	$3\alpha - \beta$	$\pi + 3\alpha - \beta$
	$s_6$	$-(3\alpha + \beta)$	$\pi - (3\alpha + \beta)$
...	...	...	...
Rays with m reflections	$s_{2m-1}$	$m\alpha + (-1)^m \beta$	$\pi + m\alpha + (-1)^m \beta$
	$s_{2m}$	$-\{m\alpha + (-1)^{m-1} \beta\}$	$\pi - \{m\alpha + (-1)^{m-1} \beta\}$

\*Real source

the positions of the virtual sources. For  $\alpha = \pi/p$  and  $\beta = 0$ , it is easily seen in Table 1 that the source and the  $2p - 1$  virtual sources are equally spaced (and separated by an angle  $\alpha$ ) around the circumference of the full sphere, as illustrated in Figure 4. If the source is moved through an angle  $\beta$ , each of the virtual sources also moves through an angle  $\beta$  and the direction of their movement can be quickly determined by following the circumference and assigning alternate directions to successive virtual sources (as indicated by the arrows in Figure 4). Since the virtual sources and the beams move through an angle equal to the source movement, the beam-factor for all beams is unity. For the case of  $p$  odd ( $= 3$ ), the source and the principal virtual source  $S_{5,6}$  move in opposite directions so that the principal beam position is  $-\beta$ . For a case of  $p$  even, say  $p = 4$ , two virtual sources are added, one to each side of the full sphere, so that the source and the principal virtual source  $S_{7,8}$  move in the same direction and the principal beam position is  $+\beta$ . It can be seen that the virtual sources and their beams move toward each other in pairs, and when  $\beta = \alpha/2$ , each of the pairs is combined into one virtual source. For these spherical wedge-shaped lenses, it can also be seen that if the source is moved toward one of the poles of the sphere (i.e., moved in a plane perpendicular to the plane in Figure 4) through an angle  $\phi$  the virtual sources also move toward the same pole through an angle  $\phi$ .

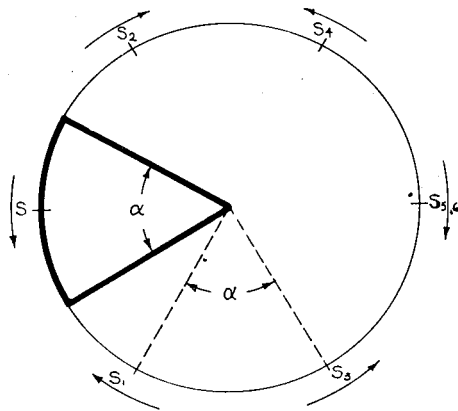


Figure 4 - Positions and directions of movement of virtual sources for  $p = 3$

containing the feed and the axis will superimpose scanning in this plane, so that volumetric scanning may be obtained.

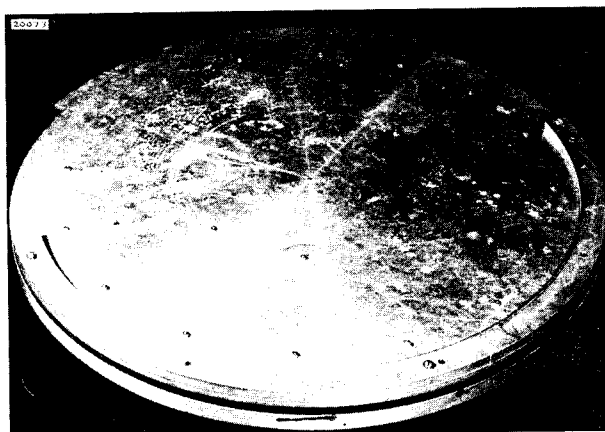
These same virtual source considerations can be applied to a spherical pyramid bounded by plane reflectors, and as a result, an increased number of reflections, virtual sources, and radiated beams will exist. In this instance, the additional parameters present in the number of reflecting planes and the angles between these planes provide such a large variety of possibilities that the development of a general system for determining positions of virtual sources and radiated beams does not seem advisable at this time.

## EXPERIMENTAL PROGRAM

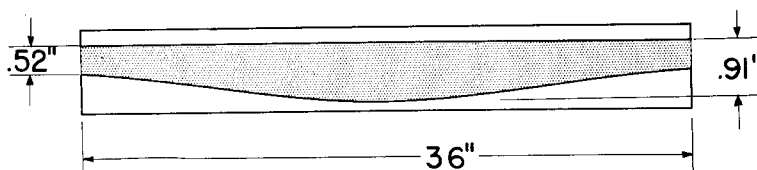
An experimental study was undertaken to determine the validity of virtual source considerations applied to the Luneberg lens and to measure the relative gain, position, beamwidth, and sidelobe level of the radiated beams. The virtual source considerations appeared quite valid, but there were some questions about the interaction of the radiated beams and the possible diffraction effects from nonsymmetrically illuminated apertures and from a high illumination appearing at a reflector edge for some feed positions.

Two methods of utilizing these lenses for scanning antennas are apparent. One method consists of rotating the feed around the circumference of a stationary lens to obtain a scan of the principal beam over an angle  $\alpha$  (or slightly less than  $\alpha$  if the gain of the unwanted beams is considered as a limiting factor). Another method, if  $p$  is odd, consists of rotating the lens past a stationary feed to obtain a scan over an angle  $2\alpha$ . If  $p$  is even, no scanning of the principal beam is obtained by this second method; this may be seen by inspecting the virtual source positions as was done in the preceding paragraph. This second method of scanning may be extended by rotating a lens composed of  $2p$  ( $p$  odd) identical virtual source lenses (i.e., a full sphere of these lenses) to obtain a sawtooth, sector scan over an angle  $2\alpha$  at the rate of  $2p$  scans per revolution of the lens. When the lens rotation produces scanning in the plane perpendicular to the rotation axis, a movement of the feed in the plane

For this study, a lens with  $\alpha = \pi$  or  $p = 1$  (Figure 2) was chosen. Ordinarily, a two-layer pillbox construction would be used to eliminate feed blocking for small feed displacements from the reference axis. In this instance, however, it was easy to obtain a virtual source lens by converting a two-dimensional Luneberg<sup>2</sup> which was composed of two circular, almost parallel plates and a polystyrene filler between the plates. The variation in  $n$  is obtained by utilizing the  $TE_{10}$  mode (E-field parallel to the plates) and varying the lens thickness, or plate spacing, with the radius. This 36-inch-diameter lens, together with a cross-sectional sketch which greatly exaggerates the plate curvature, is shown in Figure 5. Designed at 3.2 cm, it produced a 2.2 degree beamwidth E-plane radiation pattern with sidelobes 18 db below peak power when fed with a source whose illumination tapers to 18 db below peak at  $\psi = \pm \pi/2$ . By placing a reflecting surface along a diameter of this lens a virtual source lens was obtained. The reflector was made 3/16 inch in thickness to prevent energy from propagating past it. It was found experimentally that the original feed (the lower waveguide in Figure 6) when used with this virtual source lens gave too much aperture blocking for small values of  $\beta$ . However, when the 90° curved section of waveguide (Figure 6) was added so that only a small length of feed was left in the plane of the lens, aperture blocking was reduced considerably.



(a) Top view



(b) Cross-sectional view

Figure 5 - Experimental Luneberg lens

For a lens with  $\alpha = \pi$ , there is a virtual source at an angle  $\pi - \beta$  and two radiation beams, a reflected beam at  $-\beta$ , and a direct beam at  $\pi + \beta$ . The reflected beam, formed of rays with one reflection, is the principal one. Although detailed radiation-pattern calculation for these beams is impractical and somewhat unneeded, an idea of the relative gains and beamwidths may be obtained by considering the energy in the beams and the projected effective apertures from which these beams are radiated. It will be assumed that the beamwidths are inversely proportional to the relative apertures and that relative gain is proportional to both the total energy in the beam and the relative apertures. As shown in Figure 2, the projected apertures for the reflected and direct beams are  $1 + \cos\beta$  and  $1 - \cos\beta$ , respectively, for a unit-radius lens. Then, assuming a 2.2 degree beamwidth for the reflected beam

<sup>2</sup>Peeler G. D. M., and Archer, D. H., "A Two-Dimensional Microwave Luneberg Lens," NRL Report 4115, March 2, 1953

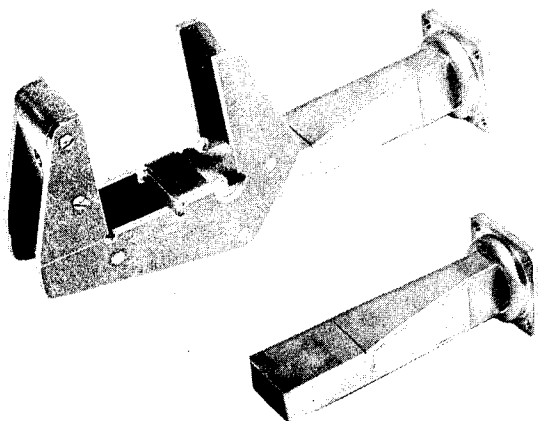


Figure 6 - Feeds for lens

when  $\beta = 0$  (as found in the full lens), the reflected-beam beamwidth should vary as  $2(2.2)/1 + \cos\beta$  and the direct-beam beamwidth as  $2(2.2)/1 - \cos\beta$ . Peeler and Archer<sup>2</sup> showed that the normalized electric field at the aperture of this lens is approximately  $|E_a| = c \cos\psi$ , where  $c$  is a constant. The integral of  $|E_a|^2$  over the projected portion of the aperture radiating a beam yields the energy in the beam, and the integral multiplied by the projected aperture gives the expected relative gain. These calculated beamwidths and relative gains are shown by the dashed curves in Figure 7. As  $\beta$  approaches  $\pm 90^\circ$  the calculated gains of the two beams become equal and are 6 db below the reflected beam gain for  $\beta = 0$  since the power becomes equally divided between the two

beams and each aperture approaches one half of the reflected beam aperture for  $\beta = 0$ . As  $\beta$  approaches  $\pm 90^\circ$ , both beamwidths approach 4.4 degrees or twice the reflected-beam beamwidth for  $\beta = 0$ .

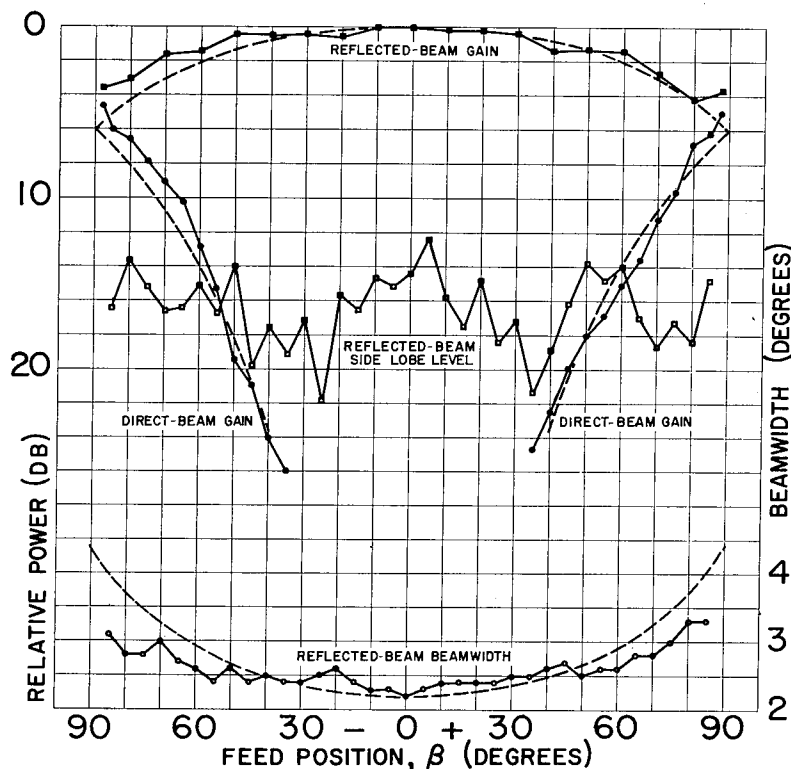


Figure 7 - Experimental and calculated data for a one-reflector virtual source lens

For comparison, Figure 7 also contains experimental data obtained from E-plane radiation patterns taken at a frequency of 9315 Mc. In plotting these data, the peak power and sidelobe level for each pattern have been normalized to the reflected-beam peak power at  $\beta = 0$ . This method permits easy comparison of the reflected-beam sidelobe level and

the direct-beam peak power. For any particular feed position, the sidelobe level is found by taking the difference between the peak power and the indicated sidelobe level. Experimental results agree quite well with calculations. The beam positions were as calculated but were not plotted. The actual beamwidth of the reflected beam is slightly greater than the calculated width for  $|\beta| < 40^\circ$  and somewhat smaller for  $|\beta| > 50^\circ$ . A sidelobe level of 14 db for the reflected beam is somewhat higher than might at first be expected; for  $|\beta| < 45^\circ$ , however, an increase in the normal sidelobe level might be expected as a result of feed blocking. For the larger  $\beta$ 's, the sidelobe level is probably due to the nonsymmetrical amplitude distribution over the reflected beam aperture. The direct-beam gain is below the sidelobe level of the reflected-beam for  $|\beta| < 55^\circ$ , and the reflected-beam gain drops only 1.4 db at the edges of this range.

It can be noticed that data taken for this lens show asymmetry which can probably be attributed to some of the slight imperfections in the model. As a result of handling, the polystyrene around several of the bolt holes has fractured somewhat so that local refraction could occur in these regions. The fit between the reflector and the polystyrene appears good but a slight separation might also give local effects. There is no apparent reason to suspect asymmetry, therefore a better model might provide symmetry and perhaps a lower sidelobe level.

For larger values of  $\beta$ , the direct-beam gain is greater than the sidelobe level of the reflected beam and could restrict the limit of operation for some applications. The direct-beam gain can be considerably reduced by placing absorbent material at the edges of the lens so that rays in the direct beam are absorbed without disturbing the rays in the reflected beam. Figure 8 shows one method of placing this material to absorb all the rays in the direct beam for  $\beta = \pm 60^\circ$ . For larger values of  $\beta$ , not all of the direct-beam rays will be absorbed, but only those rays with little energy will be radiated past the absorbers. Also, for  $|\beta| > 60^\circ$ , the gain of the reflected beam should be reduced slightly as a result of the absorption of some of its energy.

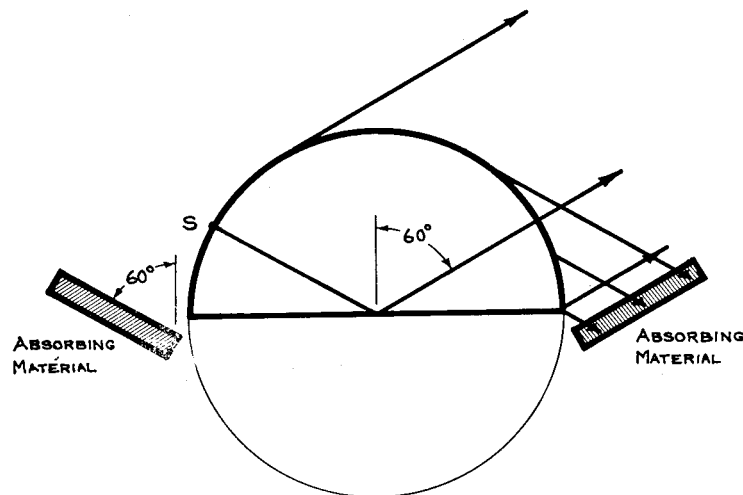


Figure 8 - One-reflector virtual source lens with absorbing material

Figure 9 contains experimental data for this lens; microwave absorbing material<sup>\*,3</sup> has been added as shown in Figure 8. The direct-beam gain was reduced below the sidelobe

\*Manufactured by the Sponge Rubber Products Co.

<sup>3</sup>Simmons, A. J., and Emerson, W. H., "An Anechoic Chamber Making Use of a New Broadband Absorbing Material," NRL Report 4193, July 1953

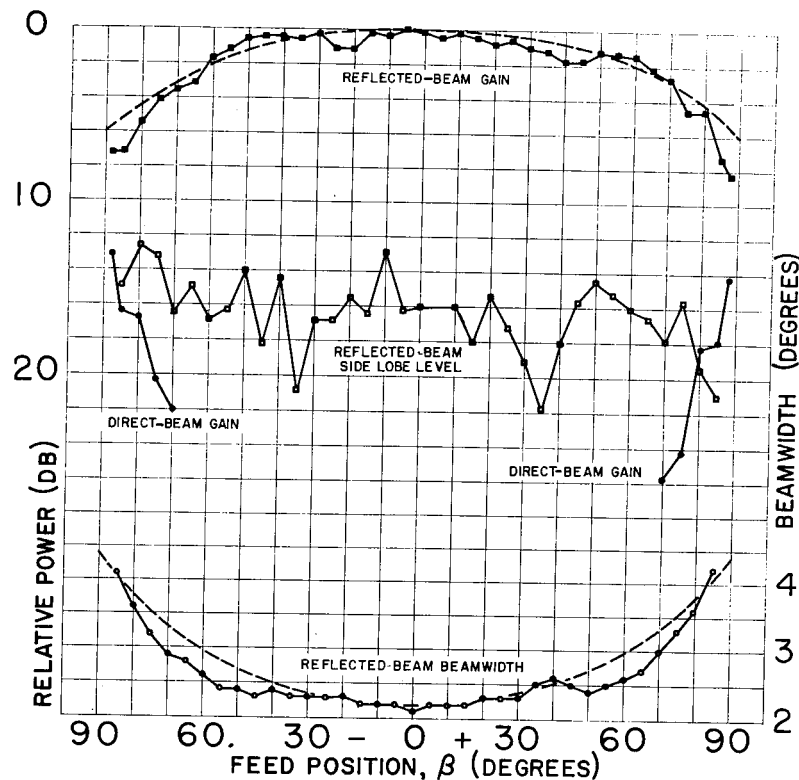


Figure 9 - Experimental data for a one-reflector virtual source lens with absorbing material

level of the reflected beam for  $|\beta| < 80^\circ$ . No effect on the reflected beam is noticed for  $|\beta| < 60^\circ$ ; both gain and beamwidth, however, deteriorated slightly for  $|\beta| > 60^\circ$ . The calculated gain and beamwidth of the reflected beam for the lens without absorbing material is included for reference.

Another method for reducing the direct-beam gain appears feasible, although it was not checked experimentally. The reflector can be extended beyond the edge of the lens so that part of the direct-beam energy is directed into the reflected beam. Since this energy is in phase with the energy already present in the reflected beam, this method should maintain the reflected-beam gain and beamwidth more constant with  $\beta$ . The extension of the reflector also serves to decrease the direct-beam gain.

The gain of unwanted beams can be further reduced by employing a greater illumination taper so that these beams contain less energy. This method has chief advantage for small values of  $\beta$ ; as  $\beta$  approaches  $\alpha/2$ , its use entails less gain reduction. For the larger  $\beta$ 's, however, tipping the feed so that the central ray is not directed at the wedge vertex would result in less energy in these beams. The use of more directive feeds is probably mandatory for small wedge-angle lenses which can produce several beams with gains comparable with the gain of the principal beam.

## SUMMARY

The analysis of virtual source Luneberg lenses shows that they can produce several perfectly focused radiation beams, each appearing to originate from a separate virtual

source. The virtual source and beam positions can be accurately predicted from the spherical wedge angle  $\alpha$  and the feed position  $\beta$ . In general, only a few of the beams are important; others contain little energy and have large beamwidth patterns so that their gain is below the diffraction sidelobe level of the important beams. For lenses with  $\alpha = \pi/p$ , where  $p$  is an integer, the beam with greatest gain has a position of  $\pm\beta$ , or has a displacement from the wedge bisector equal to that of the feed, so that this lens has a unity beam-factor.

Experimental data on a two-dimensional lens with  $p = 1$  show good agreement with calculated beam positions, gain, and beamwidth. The sidelobe level from a spherical-wedge model or from a double-layer model would probably be somewhat lower than that found with this two-dimensional lens. Several methods for reducing the gain of unwanted beams were presented, and one method involving the addition of absorbing material was verified experimentally.

If a scan angle less than  $120^\circ$  is desired, these lenses are useful for applications in which the size or weight of a full Luneberg sphere is prohibitive. For applications requiring several beams, where information from the beams need not be separated, one of these lenses can probably be designed to provide beams with the required gains in the desired directions.

\* \* \*

